J. Membrane Biol. 132, 95–113 (1993)

The Journal of
Membrane Biology

Allosterism and Na^+-D-Glucose Cotransport Kinetics in Rabbit Jejunal Vesicles: Compatibility with Mixed Positive and Negative Cooperativities in a Homo- Dimeric or Tetrameric Structure and Experimental Evidence for Only One Transport Protein Involved

Catherine Chenu and Alfred Berteloot

Membrane Transport Research Group, Department of Physiology, Faculty of Medicine, University of Montreal, Montreal, (Quebec), Canada H3C 3J7

Summary. We first present two simple dimeric models of cotransport that may account for all of the kinetics of Na^+-D-glucose cotransport published so far in the small intestine. Both the sigmoidicity in the Na^+ activation of transport (positive cooperativity) and the upward deviations from linearity in the Eadie-Hofstee plots relative to glucose concentrations (negative cooperativity) can be rationalized within the concept of allosteric kinetic mechanisms corresponding to either of two models involving sequential or mixed concerted and sequential conformational changes. Such models also allow for 2 Na^+ : 1 S and 1 Na^+ : 1 S stoichiometries of cotransport at low and high substrate concentrations, respectively, and for partial inhibition by inhibitors or substrate analogues. Moreover, it is shown that the dimeric models may present physiological advantages over the seemingly admitted hypothesis of two different cotransporters in that tissue. We next address the reevaluation of Na^+-D-glucose cotransport kinetics in rabbit intestinal brush border membrane vesicles using stable membrane preparations, a dynamic approach with the Fast Sampling Rapid Filtration Apparatus (FSRFA), and both nonlinear regression and statistical analyses. Under different conditions of temperatures, Na^+ concentrations, and membrane potentials clamped using two different techniques, we demonstrate that our data can be fully accounted for by the presence of only one carrier in rabbit jejunal brush border membranes since transport kinetics relative to glucose concentrations satisfy simple Michaelis-Menten kinetics. Although supporting a monomeric structure of the cotransporter, such a conclusion would conflict with previous kinetic data and more recent studies implying a polymeric structure of the carrier protein. We thus consider a number of alternatives trying to reconcile the observation of Michaelis-Menten kinetics with allosteric mechanisms of cotransport associated with both positive and negative cooperativities for Na^+ and glucose binding, respectively. Such models, implying energy storage and release steps through conformational changes associated with ligand binding to an allosteric protein, provide a rational hypothesis to understand the long-time debated question of energy transduction from the Na^+ electrochemical gradient to the transporter.

Key Words Na^+-D-glucose cotransport · allosteric kinetics · (dimer, tetramer) · positive and negative cooperativities · brush border membrane vesicles · rabbit jejunum

Introduction

It has been generally assumed, up to the early eighties, that Na^+-dependent D-glucose transport in mammals is homogeneous [8]. The now classical series of papers by Turner and Moran [62–64], demonstrating two, physically separable, Na^+-dependent D-glucose transport systems in the kidney, seems to have put a definitive end to that assumption [12, 54–55]. Still, the situation in the small intestine is not that clear. Indeed, kinetic evidence has accumulated over the last 10 years that is compatible with the existence of both high- and low-affinity pathways for Na^+-D-glucose cotransport in rabbit [12, 24, 27], bovine [25], guinea pig [5], rat [15], and both fetal [37–38] and adult human [16] small intestines. A major advance in the field occurred with the cloning of a rabbit intestinal cotransporter (SGLT1) [18] which was shown to correspond to a high-affinity system with stoichiometry of 2 Na^+ : 1 Glucose [47] and to present more than 99% identity with a kidney cDNA sequence [7, 42]. The availability of both cDNA probes and antibodies for that cotransporter has allowed examination of the tissue distribution of SGLT1 by in situ hybridization and immunocytochemical techniques. Such studies in the rat [58] and the rabbit [22] small intestines have failed to confirm the earlier suggestion for a physical separation of a high-affinity pathway to the villus cells and of a low-affinity pathway to the crypt cells [13–14, 26]. In the rat kidney, too, the physical separation of the low-affinity pathway to the outer cortex and of the high-affinity pathway to the outer medulla [62] has been challenged since SGLT1 has been localized to all three segments of the proximal tubule [57]. Although the possibility for isoforms of Na^+-dependent glucose transporters

could not be ruled out in these studies [57], as suggested also by indirect evidence from recent molecular biology studies in the rabbit kidney [46], it is quite apparent that the available data are not incompatible with the existence of only one transport protein. In agreement with that conclusion, at least in the small intestine, it should be noted that a single missense mutation of SGLT1 fully accounts for intestinal glucose-galactose malabsorption in human patients [59].

It seems fair to conclude that the existence of two different Na^+-D-glucose cotransporters is a hypothesis that stems from kinetic studies mostly performed using brush border membrane vesicles and showing: (i) curvilinear Eadie-Hofstee plots relative to glucose concentrations [5, 12, 15–16, 24–25, 27, 37–38, 62]; (ii) stoichiometries of 2 Na^+ : 1 Glucose and 1 Na^+ : 1 Glucose at low and high glucose concentrations, respectively [24–25, 37, 63]; and (iii) partial inhibition by a substrate analogue [19, 38] and/or inhibitor [38]. It thus becomes important at this point to question whether or not those arguments, altogether, constitute a necessary and sufficient condition in support of the existence of two different cotransporters. To state it otherwise: could these observations reflect intrinsic properties of a particular cotransport mechanism rather than a mere heterogeneity in the carrier proteins? For example, deviations from pure Michaelis-Menten kinetics in a monomeric transporter have already been discussed by reference to the so-called steady-state, (iso) random bi-bi mechanism of cotransport in which the fully loaded complex (transporter-Na^+-glucose) can be formed from either of two pathways depending on which one of the ion or the substrate binds first to the transporter [10, 17, 51, 54–55]. While such a consideration may be compatible with point (i), it cannot account for points (ii) and (iii) above. Over the past several years, too, a number of workers in the field have considered the idea that the expression of two Na^+-D-glucose transport pathways in brush border membranes may be the consequence of variations in the number and arrangement of the same set of subunits [9, 27, 30, 52, 54). In agreement with that idea, recent observations from two independent laboratories have suggested a polymeric structure of the cotransporter [31, 56], thus raising the interesting possibility for an allosteric mechanism of Na^+-D-glucose cotransport. To our knowledge, however, this hypothesis has not yet been explored in terms of cotransport kinetics.

It is clear that the hypothesis for two independent Na^+-glucose cotransporters in brush border membrane vesicles most often relies on the observation of curvilinear Eadie-Hofstee plots relative to glucose concentrations [12, 15–16, 24–25, 27, 37–38, 62). The validity of that interpretation depends on a number of experimental, theoretical, and analytical limitations which have been delineated over the last decade (4, 12, 20, 28, 43, 54, 60). Highly relevant to the context of the present discussion are the following points which result from recent studies in our group: (i) it has been generally assumed that membrane vesicles are stable with time and incubation temperatures. Our observation that rabbit and rat intestinal preparations are highly unstable [36] raises the possibility for artifactual deviations from a simple Michaelis-Menten behavior in those studies that failed to take this parameter into account; (ii) meaningful kinetic analyses performed in the presence of zero-*trans* Na^+ and substrate gradients must satisfy the initial rate assumption. In our laboratory, we have developed a fast sampling, rapid filtration apparatus (FSRFA) on the rationale that it would definitely solve the problem of initial rate measurements since allowing fast and multiple sampling from the same incubation mixture [3], true initial rates can thus be determined from uptake time courses recorded under different experimental conditions; (iii) the importance of using nonlinear instead of linear regression analysis in kinetic parameter determinations has been clearly put into focus in a paper from our group [39] where it was shown that the analytical procedures relying on the Eadie-Hofstee transformation of the uptake data, after subtracting first the nonspecific component, are endowed with a number of problems that make them unsuitable to assess the existence of more than one transport system in kinetic studies using a radiotracer technique. The best way to deal with that problem has been discussed at length in a recent review [4] and an alternative method, based on the nonlinear regression analysis of tracer uptake *vs.* cold substrate concentrations, has been proposed [39]; and (iv) on a theoretical point of view, upward deviations from linearity in Eadie-Hofstee plots may be viewed as evidence for negative cooperativity in ligand binding while sigmoid curves are compatible with positive cooperativity in effector activation [34, 44]. When applied to Na^+-D-glucose cotransport kinetics, these considerations suggest a possible reinterpretation of previous results within the concept of allosteric kinetics and form the basis of the models to be developed in the following sections.

It is thus the first aim of our paper to demonstrate that simple allosteric models may account for the kinetics of Na^+-D-glucose cotransport and may even present physiological advantages over the seemingly admitted hypothesis of two different cotransporters. Also, because of the critical role

played by Eadie-Hofstee plots in supporting that hypothesis, it is the second aim of this paper to reevaluate Na^+-D-glucose cotransport kinetics in rabbit intestinal brush border membrane vesicles using stable membrane preparations, a dynamic approach with the FSRFA, and nonlinear regression analysis. We herein demonstrate that our data can be fully accounted for by the presence of only one carrier and that this transporter follows simple Michaelis-Menten kinetics. We finally discuss a number of alternatives trying to reconcile our data with previous kinetic results [19, 24–25, 37–38, 63] and the recent suggestion of a multimeric structure of the cotransporter [31, 56].

Theory

(1) A Possible Dimeric Model for Na^+-D-Glucose Cotransport

(a) *Hypotheses*

Since two recent studies agree on a minimum number of two subunits being involved in the in situ operation of the Na^+-D-glucose cotransporter [31, 56] and since a cDNA cloned from the rabbit small intestine has been shown to produce Na^+-D-glucose cotransport activity in *Xenopus laevis* oocytes after injection of the corresponding mRNA [18, 47], it is our first hypothesis that a basic dimeric structure of the cotransporter needs to involve identical subunits (homodimer).

One may then have to decide for a number of Na^+ and glucose binding sites on each subunit. It is our second hypothesis that each subunit has two binding sites, one for Na^+ and one for substrate, as suggested by the data of Peerce and Wright [49–50].

Although not essential to our demonstration, but in accordance with some data in the current literature, and in order to simplify both the formal representation and the discussion of the models to be considered here, we also assume that: (i) Na^+ binding is a prerequisite to glucose (S) binding ([28, 47, 54] and Fig. 9); (ii) there is a maximum of two conformational changes, each being induced upon Na^+ and S binding [49–50]; and (iii) the cooperativity observed in kinetic studies is the direct result of the cooperativity in ligand binding [44].

All other assumptions made in the following three sections are similar to those usually made in deriving transport equations [61]: (i) the binding sites (of the dimer) are only accessible from one side of the membrane at a time; (ii) the reorientation (of the dimer) in the unloaded and substrate loaded states is a first-order process; (iii) the total number of (dimeric) carriers is constant; (iv) there is no net flux of (dimeric) carriers from one membrane side to the other (steady state); and (v) a rapid equilibrium in substrate binding prevails at the membrane surfaces (the reorientation steps are rate limiting).

(b) *Sequential Model*

Because of the negative cooperativity observed in glucose binding and since a concerted model of Monod et al. (MWC model) [41] can only explain positive cooperativity [34–35, 44], we first considered a generalized sequential model of Koshland et al. [32] (KNF model) as the most likely to explain Na^+-D-glucose cotransport kinetics within a dimeric structure. Such a model is shown in Fig. 1*A* and has the following characteristics: (i) the free dimer exists under a symmetrical conformation (two circles) and one Na^+ binds first to induce a conformational change (square) that allows for high-affinity glucose binding; (ii) starting from the now asymmetric dimer (square and circle), an extra Na^+ ion can bind and induce a conformational change that brings the carrier into a new symmetrical structure with two, high-affinity glucose binding sites (two squares); (iii) glucose (S) binding to either of the asymmetrical or symmetrical forms of the Na^+ activated dimers also induces a conformational change (from circle or square to triangle) in the neighboring subunit; and (iv) binding of a second substrate molecule to the two-Na^+-activated dimer gives a final, symmetrical structure of the dimer (two squares).

(c) *Validation and Basic Properties of the Dimeric Model*

Representing the diagram of Fig. 1*A* under a more conventional form used for the derivation of model equations, one gets the scheme of Fig. 1*B*. A very interesting remark is that, when not considering the lower complex $C\text{-}Na_2\text{-}S_2$, this scheme corresponds to what seems presently the most accepted sequence for the order of substrate binding [28, 54] and is in fact the one used by Kimmich [28] to elaborate his most recent model. It should be emphasized, however, that it is the presence of such a complex that may be responsible for the curvilinearity in Eadie-Hofstee plots relative to glucose concentrations. Without writing any equation, it is quite easy to understand that if $K_6 \gg K_2$ and K_4, then saturation of the first substrate site (square in Fig. 1*A*) will be almost complete before any significant substrate binding to the second site (triangle in Fig. 1*A*) can occur, and the resulting data will be

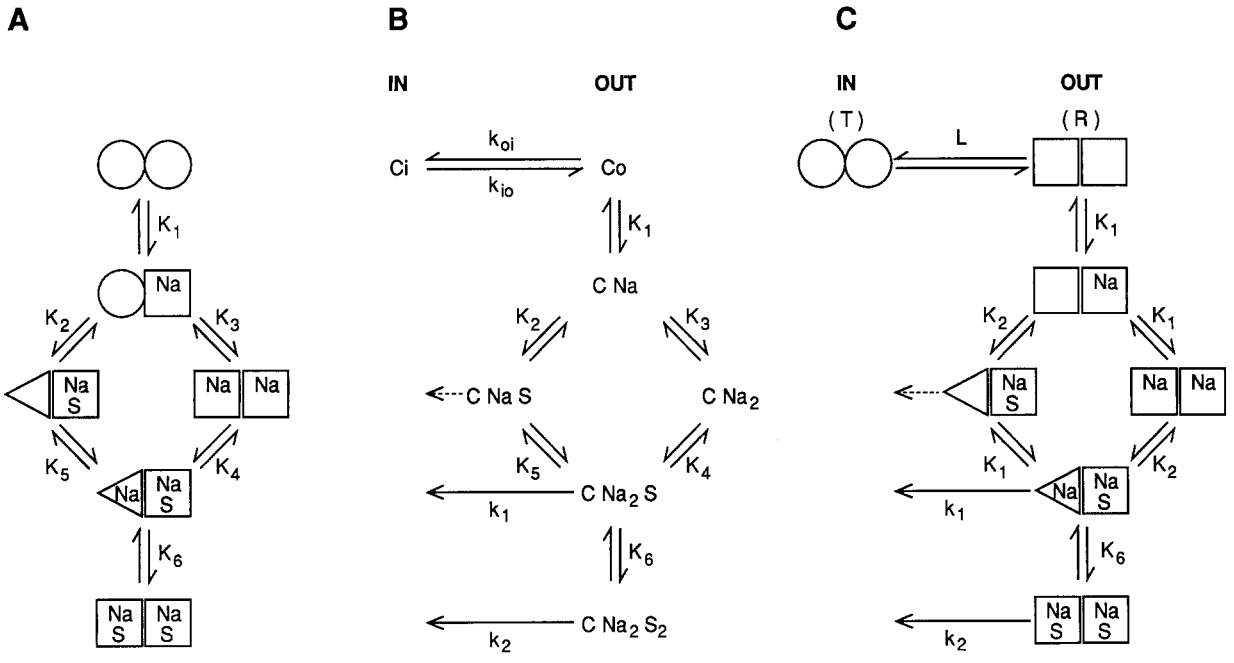

Fig. 1. Possible dimeric models for Na^+-D-glucose cotransport showing both positive cooperativity in Na^+ activation of glucose transport and negative cooperativity for substrate binding to the transporter: (*A*) Sequential model; (*B*) representation of that model according to the conventional scheme used for the derivation of rate equations; (*C*) Mixed concerted and sequential model. The K_i's are meant to represent dissociation constants (the higher their values, the lower the affinity for ligand binding). Details are given in the text.

indistinguishable from the situation expected for two different transporters. If the above inequality is not as strong, however, then the "second transporter" will not be as clearly separated, but curvilinearity in the Eadie-Hofstee plots will be maintained and negative cooperativity will be observed. As a limit case, however, weak negative cooperativity may be indistinguishable from simple Michaelis-Menten behavior.

An interesting property of the dimeric model shown in Fig. 1*A* allows us to resolve within the hypothesis of a unique transporter what would otherwise be incompatible with that hypothesis in the context of a monomeric protein, namely the occurrence of 2 Na^+ : 1 Glucose and 1 Na^+ : 1 Glucose stoichiometries at low and high substrate concentrations, respectively (24–25, 37, 63). Again, without writing down any equation, the presence of both 2 Na^+ : 1 Glucose and 2 Na^+ : 2 Glucose loaded complexes, which may allow for glucose transport, is clearly apparent from Fig. 1*A*. Obviously, the stoichiometry of the latter cannot be differentiated experimentally from a 1 Na^+ : 1 Glucose stoichiometry.

Another interesting property of the dimeric model directly understandable by visual inspection of Fig. 1*A* is that the presence of negative cooperativity in substrate binding can be best assessed under Na^+-saturating concentrations. Under these conditions, the carrier will be entirely trapped under the two-Na^+-bound form, and glucose binding will be dependent on the relative values of K_4 and K_6 only. The dimeric model should thus be easily differentiated from the steady-state, iso random bi-bi mechanism since, as shown by Sanders [51], the latter should lead to Michaelis-Menten kinetics under saturating conditions of the driver ion. It should be noted that this property of the dimeric model is compatible with data from Crane and Dorando [11] showing increased curvilinearity in the Eadie-Hofstee plots of glucose transport at high Na^+ concentrations.

A last interesting feature of the dimeric model shown in Fig. 1*A* is that it allows reevaluation of a strategy commonly used in assessing multiplicity of transport systems acting on a given substrate and which relies on the partial (competitive) inhibition by another substrate (and the implicit assumption that the transporters are monomers). Since, in the dimeric model of Fig. 1*A*, binding of one substrate molecule induces a conformational change in the substrate binding site of the neighboring subunit, such as decreasing its affinity for the binding of a second substrate molecule (negative cooperativity), it could well be then that the substrate specificity of the second site is also modified by the structural

change. Accordingly, binding of a substrate analogue to the first binding site may preclude its binding to the second site, thus producing partial inhibition only for a natural substrate.

The model of Fig. 1*A* is indeed compatible with Crane's observation that the rates of the high- and low-affinity pathways for Na^+-D-glucose cotransport are not independent as would be expected for two, totally independent, transporters [9] and with Crane's last hypothesis that the two pathways might simply represent different arrangements of subunits out of the same total pool of subunits [9]. To just give an example of how the dimeric model might provide an alternative explanation to previously published results, we will consider Malo's most recent studies on the human fetal small intestine [37–38] where the presence of two different transporters was concluded based on the following observations performed under zero-clamped membrane potential conditions: (i) nonlinearity of Eadie-Hofstee plots; (ii) stoichiometries of 2 Na^+ : 1 S and 1 Na^+ : 1 S at low and high substrate concentrations, respectively; and (iii) kinetic separation of the two transporters according to their relative specificities to 3-O-methylglucose. The picture appears quite convincing, in fact. If, however, one looks carefully to the V_{max} value in the presence of a saturating concentration of the substrate analogue (V_{max} of the so-called low-affinity system, 22 nmol · min^{-1} · mg $protein^{-1}$), it is quite surprising that it represents about half the total capacity of transport in the absence of inhibitor (33.9 + 7.5 = 41.4 nmol. min^{-1} · mg $protein^{-1}$) [38]. Such a stoichiometric ratio between the V_{max}'s of transport in the presence and absence of 3-O-methylglucose is exactly that predicted from the model of Fig. 1*B* when the rate constants for the inside to outside transitions of the 2 Na^+ : 1 *S* (k_1) and the 2 Na^+ : 2 S (k_2) loaded carriers are equal (the ligands would cross the same energy barrier during the reorientation steps). Since we have shown that points (i) and (ii) are also entirely compatible with the model of Fig. 1*A*, these studies in the human fetal small intestine [38] could as well be the best demonstration so far achieved for negative cooperativity according to that model.

(*d*) *Mixed Concerted and Sequential Model*

In the dimeric model of Fig. 1*A*, the transition from inside-facing to outside-facing conformations of the unloaded transporter has not been considered yet. To account for free carrier recycling, the KNF model of Fig. 1*A* may thus require a third conformational change for which no evidence has so far been published. The issue can be resolved, however, by considering a mixed MWC-KNF model of the type shown in Fig. 1*C* where: (i) the free carrier would exist under *T* (tight, inside-facing configuration) and *R* (relax, outside-facing conformation) forms linked through a concerted transition with dissociation constant *L* (defined as $L = [T]/[R]$); (ii) because of the symmetrical structure of the *R* form (two squares), the intrinsic affinity for the first and second Na^+ binding steps will be the same. Positive cooperativity in Na^+ binding however, will be observed since the apparent K_m for Na^+ binding to the first site will in fact be higher by a factor $(1 + L)$, compared to the apparent K_m of the second binding step [34]; and (iii) substrate binding to the 1 Na^+ and 2 Na^+ loaded forms of the transporter can now proceed as shown in Fig. 1*A*. Accordingly, negative cooperativity for substrate binding will also be observed.

While the dimeric model of Fig. 1*C* will demonstrate all of the properties described above for the dimeric model of Fig. 1*A*, it should be noted, however, that the former also allows for extra properties not yet discussed. Since the positive cooperativity in Na^+ binding entirely relies on the value of *L* (from the definition of this parameter, the higher its value, the higher the concentration of inside-facing transporter *T*, and the higher the extent of positive cooperativity), it can be anticipated that any experimental condition leading to a limit where $L \approx 0$ will tend towards a simple Michaelis-Menten curve for Na^+ activation of transport. For example, assuming a negative charge on the free carrier (or gate) like that proposed by Semenza's group [27, 54], a saturating, negative $\Delta\Psi$ should represent such an experimental situation and, indeed, little or no sigmoidicity in Na^+ activation of glucose transport has been reported under these conditions [27]. Such a model would also be compatible with recent studies of Parent et al. [47] showing that the apparent Hill number for Na^+ activation of SGLT1 has a value close to 2.0. This is the situation expected if one assumes $T \gg R$ ($L \to \infty$, i.e., the free carrier has a preferential inward configuration) in the model of Fig. 1*C*. In that case, however, and in agreement with the model of Parent et al. [48], the CNaS complex will not be present.

(2) Physiological Significance of Negative Cooperativity in the Functioning of the Na^+-D-Glucose Cotransporter

The models presented in Fig. 1 have in common a few interesting features which might be of physiological significance. The first aspect to be considered is the relevance of allosterism to (co)transport.

Clearly, the models of Fig. 1, even under these simple forms, can adapt substrate fluxes to different situations since at least three modes of transport are possible (transport through the CNaS complex, dashed arrows in Figs. 1*B-C*, was not allowed in the above considerations). From an evolutive point of view, it might be important to adapt one or another of these modes to a particular situation (whether in another tissue or another species). Since what is to be adapted here is essentially a V_{max}, the task would be rather challenging in a monomeric protein since this parameter is the composite of successive reactions. Many trials and errors might be necessary in order to modify these reactions and to arrive at the desired result. A multimeric protein offers an elegant solution to this dilemma by providing an easy means to do so, i.e., by changing one or just a few of the amino acids involved in the contact zone between the subunits such as to favor one working mode relative to another [34].

A second aspect to be considered is related to the lack of short-term induction or repression of intestinal glucose transport by its substrate, an observation which has been reported on many occasions [23]. Short-term regulation is possible, however, in the models of Fig. 1, since flux regulation would occur instantaneously according to the glucose concentration seen by the transporter. Glucose itself would thus be the signal for its own regulation. More interesting still, this adaptative flux would represent the most economical one in terms of cell energy expenditure since glucose absorption is increased while the Na^+ flux is kept at the same level. The whole scheme would thus be equivalent to an uncoupling mechanism, working with stoichiometries of 2 Na^+ : 1 S and 1 Na^+ : 1 S at lower and higher glucose concentrations, respectively.

Another interesting property of this flux regulation process is provided by the negative cooperativity in substrate binding and could well provide a basis for its understanding. Clearly, on an energetic point of view, the 2 Na^+ : 1 S stoichiometry is the most efficient one since it allows maximizing the energetic yield of the Na^+ electrochemical gradient. Accordingly, negative cooperativity would force the flux through that pathway at low glucose concentration and would allow for a maximum pumping efficiency under those conditions.

A last comment concerns the energy of subunit interactions, and could provide another basis for understanding the role of negative cooperativity in cotransport. As discussed by Levitzky [34], the intersubunit interaction energy is a negative quantity in the case of positive cooperativity and represents the extra amount of free energy which becomes available through a conformational change so that the binding improves from one binding step to the subsequent one. On the contrary, in negative cooperativity, the subunit interaction energy is a positive quantity characterized by conformational energy being released from the protein upon the first binding step, thus improving the affinity observed for that step at the expense of subsequent binding steps which now occur with diminished affinity. Applied to cotransport systems, where Na^+ binding may occur before substrate addition ([28, 47, 54] and Fig. 9), part of the energy contained in the Na^+ electrochemical gradient could be transferred to the carrier as conformational energy. Subsequent glucose binding could then allow release of part of that energy through another conformational change. The remaining issue is to understand the fate of the released energy. A possible answer to that question will be considered in the Discussion.

Materials and Methods

Materials

Rabbits were purchased from the Maple Lane Farm (Clifford, Ontario). D-[1-^{3}H(N)-D-glucose 15.5 Ci/mmol) was supplied by New England Nuclear (NEN), the BCA (bicinchoninic) protein assay kit by Pierce, unlabeled D-glucose by Sigma, phlorizin and ultrapure salts by Aldrich, and amiloride hydrochloride and scintillation cocktail (β-blend) by ICN Biomedicals. Cellulose nitrate filters (12.5 mm diameter, 0.65 μm pore size) were obtained from Micro Filtration Systems (MFS). All other chemicals were of the highest purity available. Linear and nonlinear regression analyses were performed using a commercial software (Enzfitter, R.J. Leatherbarrow, © 1987, Elsevier-Biosoft) and an IBM-AT compatible microcomputer.

Preparation of Brush Border Membrane Vesicles

The jejunum of male, 2.0–2.5 kg New Zealand white rabbits was removed and flushed with ice-cold 0.9% NaCl. The mucosa was scraped with a spatula on a cold glass plate, introduced into the homogenate media (50 mM mannitol, 2 mM Tris-HCl buffer pH 7.0, EGTA 5 mM) at a 1 : 20 ratio (w : v), and homogenized in a Waring blender for 1 min at full speed. Brush border membranes were purified in a P_2 fraction as described by Schmitz et al. [53] using 10 mM $MgCl_2$ as the precipitating agent, and the vesicles were prepared according to Hopfer et al. [21] with slight modifications as described below. The P_2 fractions, resuspended in 50 mM HEPES-Tris buffer pH 7.0 containing 0.1 mM $MgSO_4$ and either 300 or 500 mM mannitol, were frozen in liquid nitrogen. On the day of the experiment, the vesicles were thawed, resuspended in the final resuspension buffer, and prepared as a final P_4 pellet as described previously [1]. Vesicles were resuspended in the final resuspension buffer at a final protein concentration of 15–35 mg/ml. To insure stability of the preparation during the experiments, 25–50 μl aliquots of the resuspended vesicles were

frozen into liquid nitrogen until uptake assays [36]. When K^+ had to be loaded into the vesicles, the P_2 resuspension media contained 3 μM valinomycin to ensure full equilibration of the cation [36], and P_4 were resuspended in the same media lacking the ionophore unless used for membrane potential clamping. Routinely, batches of vesicles were prepared from 12–16 animals. The composition of the final resuspension buffers is indicated in the figure legends.

Uptake Assays

Na^+-dependent D-glucose uptake was determined under zero-*trans* gradient conditions of both ion and substrate using the FSRFA recently developed in our laboratory [3] which fully automatizes the rapid filtration technique of Hopfer et al. [21]. Our experiments were essentially performed as described previously in human intestinal brush border membrane vesicles [39]. For each assay, 20 or 40 μl of freshly thawed and prewarmed brush border membrane vesicles were loaded into the injector of the FSRFA. Uptake was initiated by injection, which triggers the zero-time signal and synchronization of the following steps, into 480 or 460 μl of uptake medium thermostated at 20°C or 35°C in the incubation chamber of the apparatus. The composition of the different incubation media is described in the figure legends. Sequential sampling of nine aliquots of the uptake mixture (50 μl each) was performed at 0.5 or 0.3 sec intervals for each of the above temperatures, respectively. The sampled aliquots were recuperated into the upper chamber of the manifold array which contained 1 ml ice-cold stop solution (50 mM HEPES-Tris buffer pH 7.0, 1 mM phlorizin, and NaCl and mannitol concentrations to match the ionic strength and the osmolarity of the different uptake assays, respectively). Filtration of the resulting mixture and two 1-ml washes with ice-cold stop solution were sequentially and automatically performed (20-sec duration). Filters were dissolved in mini-vials by 20-min incubation with 5 ml β-blend under constant agitation. Radioactivity was determined using a Minaxi Tri-Carb Series 4000, model 4450 scintillation counter (United Technologies Packard).

Under the conditions of our uptake assays, it was demonstrated that the initial rates of 50 μM D-glucose uptake were linear with protein concentrations over the range 1–35 mg protein/ml (*results not shown*). Protein was measured with the BCA assay kit using bovine serum albumin as standard.

Data Analysis

Initial Rate Determinations

The initial rates of transport were determined by linear and/or polynomial regression of the uptake time courses as justified in the Results. In the latter case, a second-order polynomial was used and the initial rates were then taken as the first-order coefficient (zero-time derivative) [4, 12]. This procedure seems justified since it is independent of the transport mechanism involved [4, 12]. For each substrate concentration used in the different experiments of Figs. 3–8, five uptake time courses were run. The glucose uptake values were averaged out at each time point, and the standard deviations of the mean values were used as weighting factors in the linear and/or polynomial regression of the uptake time courses.

Kinetic Analyses

Three different models were chosen and systematically tested under each experimental condition. Model 1 assumes transport through one transporter, so that the initial rate equation ($v = f(S)$) can be described by the classical Michaelis-Menten equation (kinetic parameters V_{max} and K_m representing the maximum transport rate and the apparent affinity for substrate binding, respectively). Model 2 assumes the existence of two different transporters, a situation most often difficult to distinguish from the steady-state, iso random bi-bi transport mechanism. Accordingly, the initial rate equation for such situations can, in general, be described by the sum of two Michaelis-Menten terms [51]. Finally, model 3 assumes the presence of only one transporter with n substrate binding sites that may show either positive or negative cooperativity in S binding. In such cases, the simplest initial rate equation corresponds to the Hill equation and the Hill number (n_H) will assume any value from 0 to n that verifies $0 < n_H \leq n$. It should be noted that this last model can also be used as a confirmatory test in support of model 1 for which a n_H value of 1.0 should be obtained. In all three models, the contribution of a simple diffusional component to the overall initial rate of substrate transport was also assumed by introducing into the rate equations above a linear term in addition to the specific Michaelian terms (diffusion rate constant k_D).

The dependence of initial transport rates on total substrate concentrations (S) were analyzed from displacement curves using nonlinear regression analysis as described recently [39]. Equation (1) was used to derive the mathematical expressions of the initial rates of tracer uptake v^* for models 1–3.

$$v^* \left[\frac{(S_{cold} + T)}{T}\right] = v = f(S, V_{max}, K_m, n_H, k_D) \tag{1}$$

In that equation, T and S_{cold} stand for tracer and cold substrate concentrations, respectively, and verify Eq. (2)

$$S = S_{cold} + T. \tag{2}$$

It should be noted that the left-hand side of Eq. (1) is equivalent to the calculation which is usually done to transform the uptake data from cpm to pmol or nmol of accumulated substrate since the raw cpm values (equivalent to v^*) are corrected for the isotopic dilution of tracer (equivalent to the term under []). The following equations were thus obtained:
Model 1:

$$v^* = \frac{V_{max} * T}{K_m + S_{cold} + T} + k_D * T \tag{3}$$

Model 2:

$$v^* = \frac{V_{max1} * T}{K_{m1} + S_{cold} + T} + \frac{V_{max2} * T}{K_{m2} + S_{cold} + T} + k_D * T \tag{4}$$

Model 3:

$$v^* = \frac{V_{max} * T * (S_{cold} + T)^{n_H - 1}}{K_m^{n_H} + (S_{cold} + T)^{n_H}} + k_D * T \tag{5}$$

All three equations are suitable for nonlinear regression analysis of the displacement curves when T is taken as a prompt constant and S_{cold} as the variable. The following remarks however apply: (i) Eq. (3–5) gave the same parameter values as those

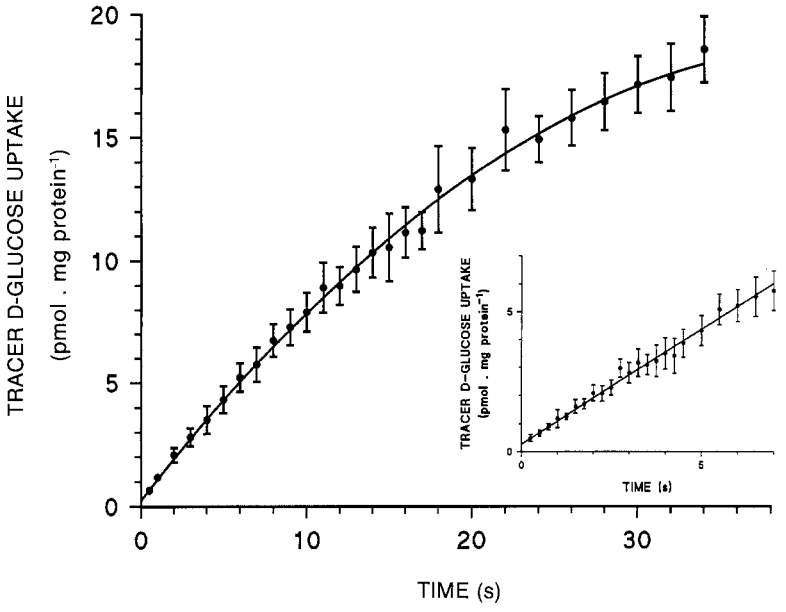

Fig. 2. Typical uptake time course of tracer D-glucose uptake. Vesicles were resuspended in 50 mM HEPES-Tris buffer (pH 7.0) containing 0.1 mM $MgSO_4$ and 200 mM KI. The uptake media contained (final concentrations): 50 mM HEPES-Tris buffer (pH 7.0), 150 mM NaI, 50 mM KI, 0.5 mM amiloride, and 4 μM D-(^{3}H)glucose. Points shown are the mean ± SD of five determinations. Inset: initial linearity in the uptake time course. The lines shown are the best fit to the data points as obtained by polynomial (main graph, $y = a_0 + a_1 * t + a_2 * t^2$) and linear (inset, $y = a * t + b$) regression analysis. Values of the parameters are: a_0, 0.24 ± 0.02; a_1, 0.86 ± 0.01; a_2, $-9.94 * 10^{-3} \pm 4.07 * 10^{-4}$; a, 0.82 ± 0.01; b, 0.27 ± 0.02.

estimated from the more classical v over S plots and the direct equations provided that equivalent weighting routines were used. The advantages in using the displacement curves, however, have been discussed previously [4, 39] and will not be repeated here; and (ii) the graphical representation of the data has been improved by plotting v^* *vs.* S instead of S_{cold} in order to avoid the break in the x axis (shown as a log scale) which was inherent to the former representation [39].

Statistical Analysis

The standard errors of regression (σ) resulting from the initial rate determinations were used as weighting factors ($1/\sigma^2$) for the nonlinear regression analysis of the v^* over S data using Eqs. (3–5). A robust weighting routine was also introduced to minimize the influence of outliers.

The goodness of fit for each model and the discrimination between rival models was based on the four criteria defined by Mannervick [40]. A model was rejected when: (i) it failed to give convergence; (ii) it gave unreasonable (for example negative) or unreliable (SD ≥ 50% of parameter value) parameter values; (iii) it showed a nonrandom distribution of the residuals; and (iv) for models surviving these three steps, the best one was chosen by considering the statistical significance of the improvement when going from model (i) to model (j) having P_i and P_j parameters ($P_j > P_i$). A F-test was thus performed according to Eq. (6)

$$F(P_j - P_i, N - P_j) = \frac{Q_i^2(N - P_i) - Q_j^2(N - P_j)}{Q_j^2(P_j - P_i)} \quad (6)$$

where Q^2 represents the mean sum of squares obtained from each model and is defined as the residual sum of squares divided by the difference between the number of data points (N) and the number of parameters (P) in the model. When the F calculated by Eq. (6) is higher than the tabulated F with the same degree of freedom, the null hypothesis (no improvement at the level $P \leq 0.05$) can be rejected and the model containing the larger number of parameters is usually favored.

Results

Initial Rate Determinations

When analyzing the uptake time courses using a linear regression routine under the set of experimental conditions described in this paper, it clearly appeared: (i) that linearity over a pre-fixed time range may not apply to all experimental conditions, even within the same experiment; and (ii) that the fair appraisal of linearity *vs.* nonlinearity over short time ranges is not necessarily a simple matter. The experiment described in Fig. 2 was then undertaken in order to: (i) test the validity of using a polynomial regression routine for the determination of initial transport rates under conditions where linearity is not observed. Although previously applied in a few laboratories [2, 12], it should be noted that the approach has been recently challenged [4, 54] on the grounds that it has never been justified for uptake studies; and (ii) define rigorous criteria that should allow assessment of deviation from linearity within a set of experimental conditions.

Figure 2 should be viewed as a typical time course of D-glucose uptake. Clearly, linearity is not observed over the whole time range (0–34 sec), but the uptake time course can be well described using a second degree polynomial (*see* equation in the legend to Fig. 2). The initial rate can thus be determined from the slope of the tangent at 0 time which is given by the first degree coefficient of the polynomial (0.860 ± 0.010 pmol · mg protein^{-1}). The initial linearity period was then estimated by linear regression to the data points and curve peeling until a

Table. Initial rate estimation using linear or polynomial regression

Time courses	Linear regression		Polynomial regression	
	Rate (*intercept*)	Q^2	Rate (*intercept*)	Q^2
1–9 sec	0.77 ± 0.01	0.0311	0.82 ± 0.05	0.0307
(n = 9)	(*0.47 ± 0.05*)		(*0.39 ± 0.09*)	
2–18 sec	0.69 ± 0.02	0.1595	0.86 ± 0.04	0.0404*
(n = 9)	(*0.79 ± 0.13*)		(*0.39 ± 0.12*)	
4–32 sec	0.53 ± 0.03	0.6665	0.83 ± 0.02	0.0112*
(n = 8)	(*2.11 ± 0.47*)		(*0.35 ± 0.10*)	

The uptake time course of Fig. 2 was divided into three sets of data, each containing 8 to 9 points equally spaced over the time scales shown in the Table. Linear and polynomial regression analyses were then performed on each set of data using the equations shown in the legend to Fig. 2. The Q^2 values represent the mean sum of squares as defined in Materials and Methods.
* Indicates a significant improvement at the 95% confidence level of the polynomial *vs.* the linear regression analysis.

constant slope value was reached. As shown in the inset of Fig. 2, linearity in the uptake time course extended up to 7 sec under these experimental conditions. A true initial rate of 0.817 ± 0.012 pmol · mg protein^{-1} can thus be determined, a value nonsignificantly different at the 95% confidence level from that obtained using polynomial regression.

While validating the polynomial regression approach to initial rate determinations when using a high number of data points, it should be stressed that the experimental design of Fig. 2 departs quite significantly from that used in the kinetic experiments described below where only nine time points were used. In order to assess the validity of the polynomial regression approach using a smaller number of data points, the uptake time course of Fig. 2 was divided into three sets of nine points each, but covering different time scales (*see* Table), and both linear and polynomial regressions were performed over these time ranges. As shown in the Table: (i) using linear regression, the initial rate values decrease when increasing the time range of the observation, in agreement with the nonlinearity in the uptake time course over the whole time range; and (ii) in all cases, polynomial regression was successful in determining the true initial rate of transport.

The Table also gives insights as to the criteria to be used in assessing linearity *vs.* nonlinearity in uptake time courses when analyzing a set of experimental conditions. Assuming that the three data sets in the Table represent uptake time courses obtained in one experiment over the same time range but under different experimental conditions (like changes in substrate concentrations in the following experiments), it is quite clear then: (i) that nonlinearity can be best assessed from a change in the y axis intercepts when applying a linear regression routine to these different conditions; (ii) that the significance in fit improvement when going from linear to polynomial regression can be evaluated from the Q^2 values using the general approach aimed at model discrimination as described under Materials and Methods, and (iii) that a constant y intercept value in the polynomial, as opposed to the linear fit, is a good diagnostic as to the assessment that nonlinearity in the uptake time courses was the only problem at hand in these experiments.

It should be noted that this procedure was systematically followed in the experiments to be now described in order to warrant an analysis of true initial rate data.

Na^+-D-Glucose Cotransport under Standard Conditions

The dependence of the initial rates of tracer D-glucose (4 μM) transport upon increasing cold substrate concentrations is shown in Fig. 3. Fitting the one-site model to the data points results in a random distribution of the residuals (inset of Fig. 3). The following observations can also be made: (i) a finite value is obtained at very high substrate concentrations, thus showing the presence of a purely passive diffusional component in transport [4, 39]; (ii) this noise level represents less than 5% of the dynamic range over which the variations in initial rates were recorded; and (iii) the difference between the initial rates measured at 10 and 200 mM substrate concentrations is in the range of the noise level so that no useful information would be gained by varying substrate concentrations over that range. Our attempts to fit the two-sites model failed to give convergence. Fitting the Hill n-sites model gave a Hill number (n_H) of 1.03 ± 0.03 with kinetic parameters values (V_{max}, 95 ± 4 pmol. mg protein^{-1} · sec^{-1}; K_m, 0.121 ± 0.020 mM; k_D, 8.0 ± 1.1 pmol. mg protein^{-1} · sec^{-1} · mM^{-1}) not significantly different from those obtained by regression to the one-site model (*see* legend to Fig. 3).

In the above experiment, iodide was used to clamp the membrane potential at 0 mV, as suggested by Berteloot [2] a few years ago. It should be noted, however, that results similar to those of Fig. 3 were obtained using K^+/valinomycin (n_H = 0.95 ± 0.02).

Experiments similar to those of Fig. 3 were performed using D-galactose as substrate. As shown in

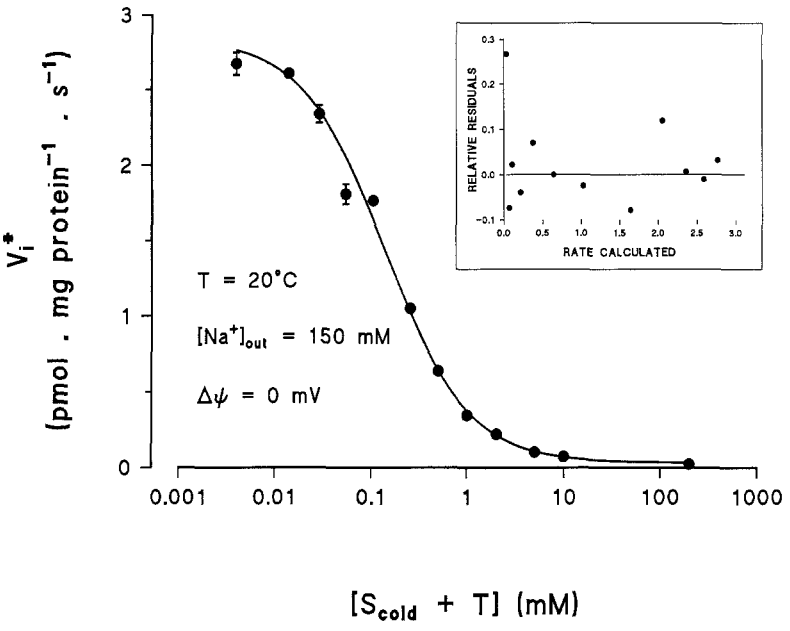

Fig. 3. Displacement curve for D-glucose transport under standard conditions. Vesicles were resuspended in 50 mM HEPES-Tris buffer (pH 7.0) containing 0.1 mM $MgSO_4$, 200 mM KI, and 300 mM mannitol. The uptake media contained (final concentrations): 50 mM HEPES-Tris buffer (pH 7.0), 150 mM NaI, 16 mM KI, 34 mM choline iodide, 0.5 mM amiloride, 4 μM D-(^{3}H)glucose, and 0–200 mM cold D-glucose. Osmolarity was kept constant by varying mannitol concentrations to satisfy a total concentration of glucose + mannitol of 300 mM. Values shown are means ± SD of five determinations performed on the same vesicle preparation. Missing error bars were smaller than the symbol size. The line shown is the best-fit curve corresponding to the one-site model (Eq. (1) in Materials and Methods). Values of the parameters are: V_{max}, 98 ± 3 pmol · mg protein^{-1} · sec^{-1}; K_m, 0.139 ± 0.005 mM; k_D, 7.6 ± 1.1 pmol · mg protein^{-1} · sec^{-1} · mM^{-1}. Inset: residual plot of the regression.

Fig. 4 using the Eadie-Hofstee representation for clear visual appraisal [4]: (i) both glucose and galactose kinetics are compatible with a simple Michaelian behavior in accordance with the above one-site model; and (ii) glucose and galactose transport differed by their apparent affinity for the carrier only, with K_m values of 0.139 ± 0.005 and 0.406 ± 0.023 mM, respectively.

Effect of Lowering External Na^+ Concentration to 60 mM

It has been argued that the steady-state, random bi-bi model of substrate addition may induce deviations from a pure Michaelian behavior in a one-site, monomeric transporter [4, 9, 17, 51, 54]. Such a model was recently considered on a theoretical basis by Sanders [51] who concluded that a simple Michaelian behavior is expected under saturating concentrations of the driving ion. Accordingly, the failure of model 2 to describe our results under standard conditions might be related to this phenomenon since the Na^+ concentration relative to its reported K_m for the glucose cotransport system was quite high in that experiment [12, 24]. This hypothesis was thus investigated by lowering the outside Na^+ concentration down to 60 mM and the results are shown in Fig. 5. It can be clearly appreciated from the regression line and the Eadie-Hofstee transformation of the data (inset of Fig. 5) that the one-site model still adequately describes these new experimental data. It should be stressed that the two-sites model failed to give convergence and that the Hill n-sites model confirmed the simple Michaelian behavior with n_H = 0.98 ± 0.02. It should also be noted that the kinetic parameters values (V_{max}, 112 ± 9 pmol · mg protein^{-1} · sec^{-1}; K_m, 0.324 ± 0.057 mM; k_D, 17.2 ± 1.7 pmol · mg protein^{-1} · sec^{-1} · mM^{-1}) for that model are not significantly different from those obtained by regression to the one-site model (*see* legend to Fig. 5).

Effect of a Negative Membrane Potential

Kinetic studies performed in other laboratories have shown heterogeneity in glucose cotransport under conditions of negative membrane potential [12]. The effect of this parameter was evaluated in our vesicle preparation using iodide to clamp the membrane potential at ≈ −69 mV (calculated from the Goldman equation as described previously [2]). Figure 6 shows the regression line and the Eadie-Hofstee transformation of the data (inset) corresponding to the one-site model. Again, the two-sites model failed to converge, and the analysis according to the Hill n-sites model (n_H = 0.96 ± 0.02) strengthens the conclusion as to a simple Michaelian behavior under these experimental conditions. Also, the kinetic parameter values (V_{max}, 305 ± 12 pmol · mg protein^{-1} · sec^{-1}; K_m, 0.130 ± 0.15 mM; k_D, 13.0 ± 3.0 pmol · mg protein^{-1} · sec^{-1} · mM^{-1}) for that model are not significantly different from those obtained by regression to the one-site model (*see* legend to Fig. 6).

In a recent review, Kimmich [28] has simulated

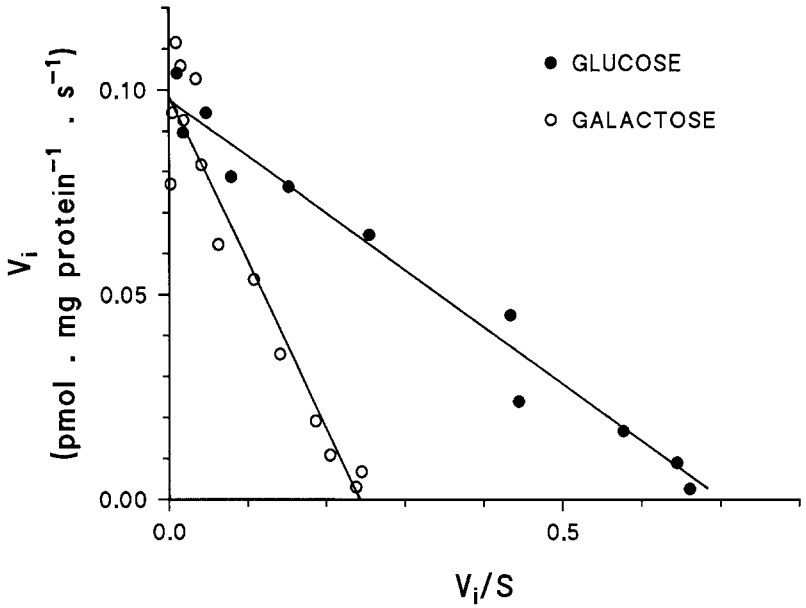

Fig. 4. Eadie-Hofstee plot of D-glucose and D-galactose transport. Experimental conditions were as described in the legend to Fig. 3. The kinetic parameters for D-glucose transport are as given in the legend to Fig. 3. The corresponding values for D-galactose transport were: V_{max}, 99 ± 5 pmol · mg protein^{-1} · sec^{-1}; K_m, 0.406 ± 0.023 mM; k_D, 6.4 ± 0.7 pmol · mg protein^{-1} · sec^{-1} · mM^{-1}.

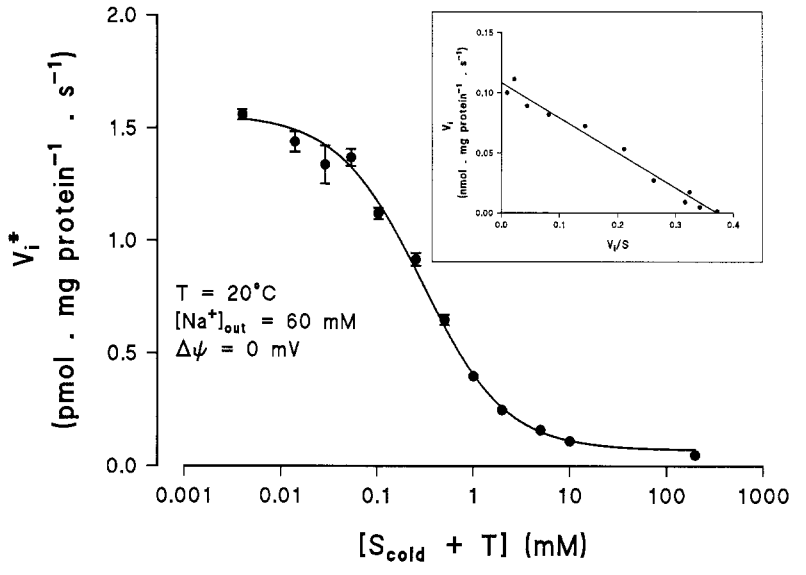

Fig. 5. Displacement curve for D-glucose transport at low Na^+ concentration. Vesicles were resuspended in 50 mM HEPES-Tris buffer (pH 7.0) containing 0.1 mM $MgSO_4$, 300 mM mannitol, and 200 mM KI. The uptake media contained (final concentrations): 50 mM HEPES-Tris buffer (pH 7.0), 0.1 mM $MgSO_4$, 60 mM NaI, 16 mM KI, 124 mM choline iodide, 0.5 mM amiloride, 4 μM D-(^{3}H)glucose, and 0–200 mM cold D-glucose. Osmolarity was kept constant by varying mannitol concentrations to satisfy a total concentration of glucose + mannitol of 300 mM. Values shown are means ± SD of five determinations performed on the same vesicle preparation. Missing error bars were smaller than the symbol size. The line shown is the best-fit curve corresponding to the one-site model (Eq. (1) in Materials and Methods). Values of the parameters are: V_{max}, 108 ± 6 pmol · mg protein^{-1} · sec^{-1}; K_m, 0.291 ± 0.020 mM; k_D, 17.7 ± 1.5 pmol · mg protein^{-1} · sec^{-1} · mM^{-1}. Inset: Eadie-Hofstee plot of the data.

the effect of uncontrolled variations in the membrane potential upon adding cold substrate concentrations and shown that it could be responsible for artifactual deviations from a Michaelian behavior. Although not supported by the above results, this possibility was investigated in our system and the membrane potential was clamped to a negative value by using a double clamping system of the type used by Kimmich et al. [29]. Using both iodide as a highly permeant anion [2] and K^+-valinomycin, the membrane potential was clamped at approximatively −53 mV as determined from the Goldman equation and the relative ionic permeabilities used or determined previously [2]. Results similar to those of Fig. 6 were obtained (n_H = 0.99 ± 0.02).

Finally, in a series of experiments reported by Crane and Dorando [11], it was shown that the curvilinearity in the Eadie-Hofstee plots was increased under negative membrane potential conditions by increasing the external Na^+ concentration up to 500 mM. These experimental conditions were thus tested and the results of this experiment are shown in Fig. 7. Again, the one-site model fairly describes those data (*see* kinetic parameters in the legend to Fig. 7), as confirmed by the analysis with the Hill *n*-sites model (n_H, 0.99 ± 0.03; V_{max}, 232 ± 15 pmol ·

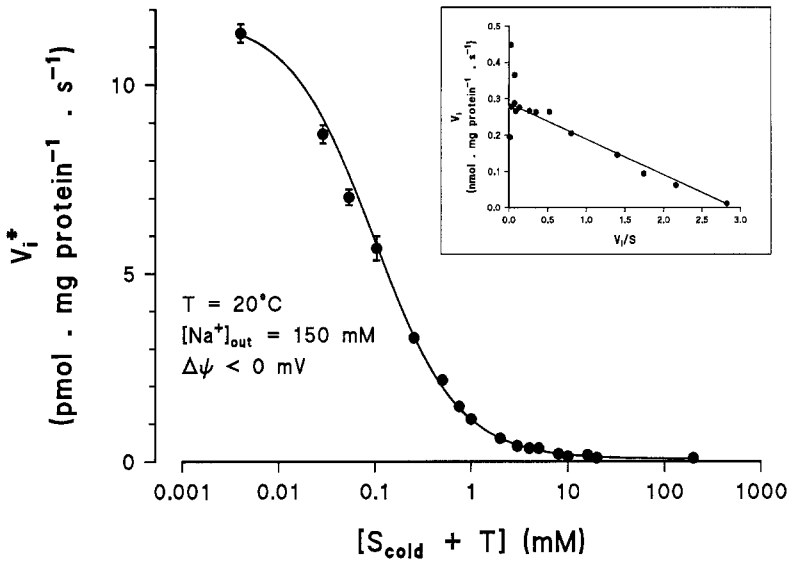

Fig. 6. Displacement curve for D-glucose transport at negative membrane potential ($\Delta\Psi$). Vesicles were resuspended in 50 mM HEPES-Tris buffer (pH 7.0) containing 0.1 mM $MgSO_4$, 300 mM mannitol, and 200 mM KCl. The uptake media contained (final concentrations): 50 mM HEPES-Tris buffer (pH 7.0), 0.1 mM $MgSO_4$, 150 mM NaI, 16 mM KCl, 34 mM choline iodide, 0.5 mM amiloride, 4 μM D-(^{3}H)glucose, and 0–200 mM cold D-glucose. Osmolarity was kept constant by varying mannitol concentrations to satisfy a total concentration of glucose + mannitol of 300 mM. Values shown are means ± SD of five determinations performed on the same vesicle preparation. Missing error bars were smaller than the symbol size. The line shown is the best-fit curve corresponding to the one-site model (Eq. (1) in Materials and Methods). Values of the parameters are: V_{max}, 287 ± 11 pmol · mg protein^{-1} · sec^{-1}; K_m, 0.098 ± 0.004 mM; k_D, 16.0 ± 3.0 pmol · mg protein^{-1} · sec^{-1} · mM^{-1}. Inset: Eadie-Hofstee plot of the data.

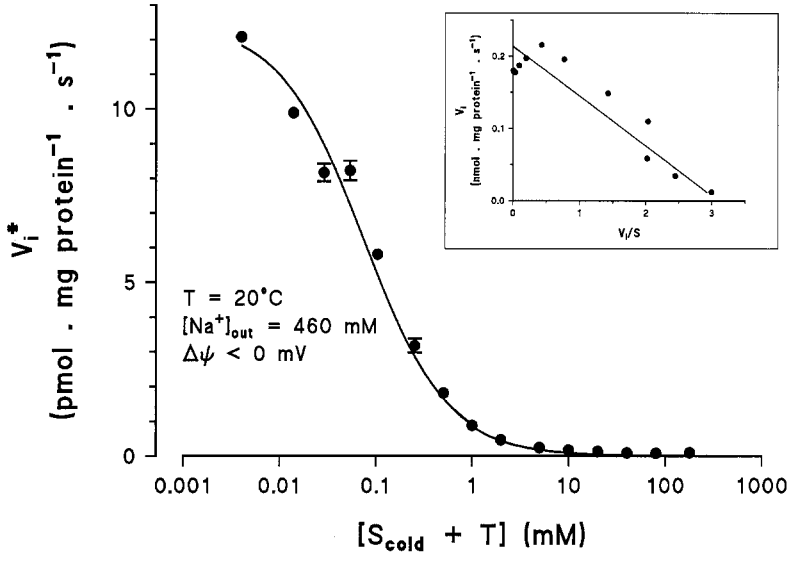

Fig. 7. Displacement curve for D-glucose transport at negative membrane potential ($\Delta\Psi$) and high Na^+ concentration. Vesicles were resuspended in 50 mM HEPES-Tris buffer (pH 7.0) containing 0.1 mM $MgSO_4$, 200 mM mannitol, and 500 mM KCl. The uptake media contained (final concentrations): 50 mM HEPES-Tris buffer (pH 7.0), 0.1 mM $MgSO_4$, 460 mM NaI, 40 mM KCl, 0.5 mM amiloride, 4 μM D-(^{3}H)glucose, and 0–180 mM cold D-glucose. Osmolarity was kept constant by varying mannitol concentrations to satisfy a total concentration of glucose + mannitol of 200 mM. Values shown are means ± SD of five determinations performed on the same vesicle preparation. Missing error bars were smaller than the symbol size. The line shown is the best-fit curve corresponding to the one-site model (Eq. (1) in Materials and Methods). Values of the parameters are: V_{max}, 229 ± 11 pmol · mg protein^{-1} · sec^{-1}; K_m, 0.074 ± 0.005 mM; k_D, 15.8 ± 3.5 pmol · mg protein^{-1} · sec^{-1} · mM^{-1}. Inset: Eadie-Hofstee plot of the data.

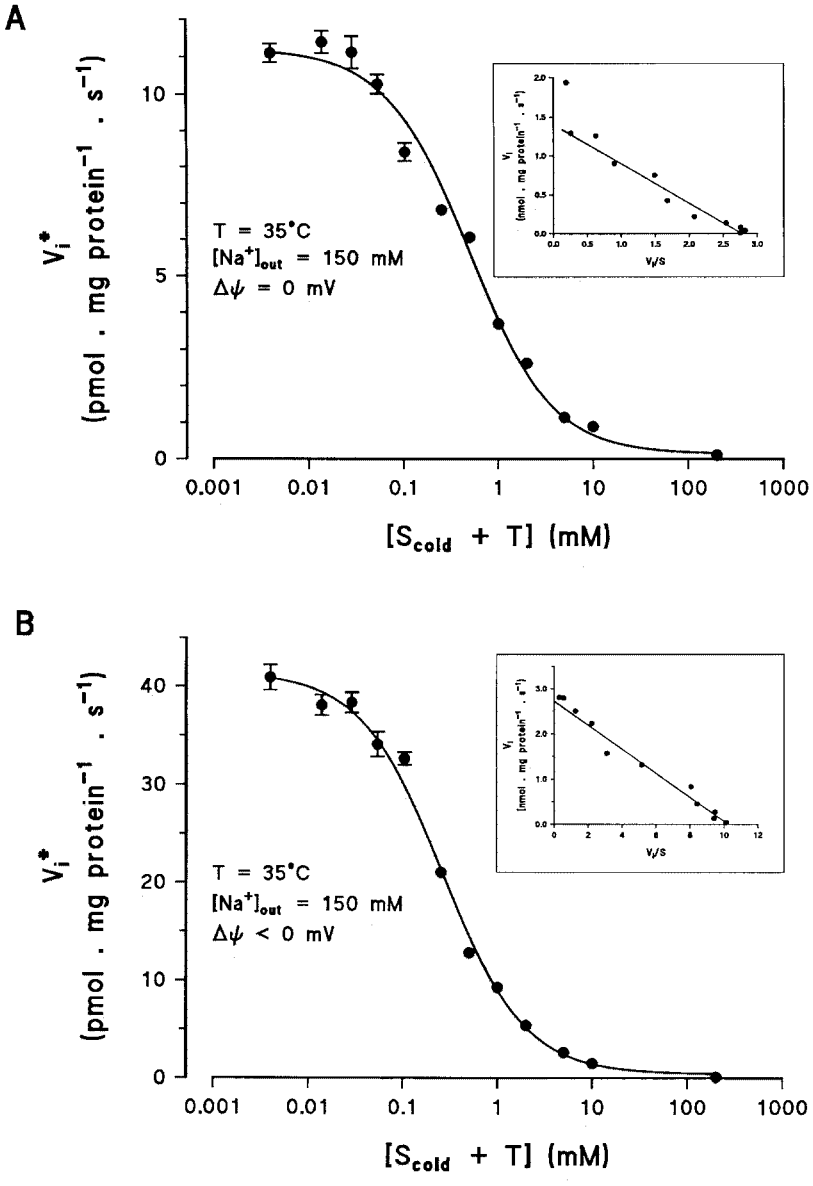

Fig. 8. Displacement curve for D-glucose transport at high temperature under conditions of 0 mV-clamped (*A*) and negative (*B*) membrane potential ($\Delta\Psi$). Experimental conditions were as described in the legends to Figs. 3 and 6. Values shown are means ± SD of five determinations performed on the same vesicle preparation but *A* and *B* correspond to different membrane preparations. Missing error bars were smaller than the symbol size. The lines shown are the best-fit curves corresponding to the one-site model (Eq. (1) in Materials and Methods). Values of the parameters are: (*A*) V_{max}, 1379 ± 135 pmol · mg protein^{-1} · sec^{-1}; K_m, 0.498 ± 0.053 mM; k_D, 33 ± 23 pmol · mg protein^{-1} · sec^{-1} · mM^{-1}; and (*B*) V_{max}, 2718 ± 127 pmol · mg protein^{-1} · sec^{-1}; K_m, 0.265 ± 0.017 mM; k_D, 101 ± 26 pmol · mg protein^{-1} · sec^{-1} · mM^{-1}. Insets: Eadie-Hofstee plot of the data.

mg protein^{-1} · sec^{-1}; K_m, 0.081 ± 0.018 mM; k_D, 15.4 ± 3.9 pmol · mg protein^{-1} · sec^{-1} · mM^{-1}) and the failure of the two-sites model to converge.

Temperature Effects

Recent studies in the guinea pig have reported a temperature-sensitive induction of a second glucose transporter [5]. We have considered this possibility in rabbit intestinal brush border membrane vesicles by increasing the temperature to 35°C under conditions of both zero-clamped and negative membrane potentials with 150 mM outside Na^+ concentrations.

Figure 8*A* ($\Delta\Psi$ = 0) and *B* ($\Delta\Psi$ < 0) shows the compatibility of the initial rate data with the one-site model, in agreement also with the analysis using the Hill *n*-sites model (at $\Delta\Psi$ = 0 and < 0 mV, respectively: n_H, 0.97 ± 0.02 and 1.10 ± 0.03; V_{max}, 1535 ± 211 and 2680 ± 97 pmol · mg protein^{-1} · sec^{-1}; K_m, 0.621 ± 128 and 0.254 ± 0.043 mM; k_D, 26 ± 26 and 103 ± 30 pmol · mg protein^{-1} · sec^{-1} · mM^{-1}). In both cases, too, the two-sites model failed to converge.

Na^+-Dependency of Na^+-D-Glucose Cotransport

So far, all of our experiments have been performed under Na^+-gradient conditions and have shown incompatibility with the two-sites and/or the Hill *n*-

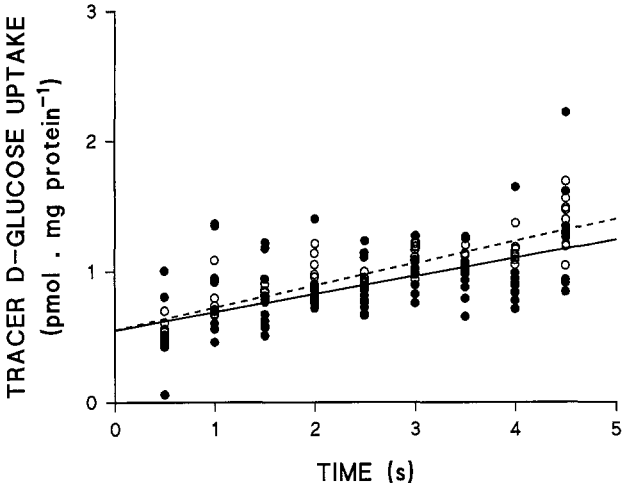

Fig. 9. Na^+ dependency of glucose transport. Vesicles were resuspended in 50 mM HEPES-tris buffer (pH 7.0), 0.1 mM $MgSO_4$, 300 mM mannitol, and 200 mM KI. The uptake media contained (final concentrations): 50 mM HEPES-tris buffer (pH 7.0), 0.1 mM $MgSO_4$, 150 mM NaI, 50 mM KI, 100 mM mannitol, 0.5 mM amiloride, 4 μM D-(^{3}H) glucose and 200 mM glucose (●, ———) or 150 mM choline iodide, 50 mM KI, 300 mM mannitol, 0.5 mM amiloride, 4 μM D-(^{3}H)glucose and 50 μM glucose (○, ----). Ten uptake time courses were run under each of the above experimental conditions. The linear regression lines ($y = a * t + b$) shown are the best-fit lines over all individual data points in each experiment. Regression parameters: a (pmol · mg protein^{-1} · sec^{-1}), 0.130 ± 0.018 (●), 0.169 ± 0.009 (○); and b (pmol · mg protein^{-1}), 0.543 ± 0.049 (●), 0.543 ± 0.026 (○).

sites models of cotransport. It has been shown, however, that glucose transport may occur in the complete absence of Na^+ [5, 6, 12]. In order to definitely assess whether D-glucose transport in rabbit jejunum has an obligatory requirement for Na^+, we have measured: (i) tracer D-glucose (4 μM) uptake in the presence of 150 mM Na^+ and saturating concentration of D-glucose (200 mM) which should give a reliable estimate of the passive diffusional component of glucose transport (*see* Figs. 3–8); and (ii) tracer D-glucose uptake in the presence of 50 μM cold glucose and 150 mM choline which should provide high sensitivity in measuring any carrier-mediated component of glucose transport in the absence of Na^+. Moreover, to increase the signal over noise (S/N) ratio of the assay, this experiment was performed at 35°C (*see* Fig. 8*A*) and 10 independent measurements were made under each of these two conditions. The results of these experiments are reported in Fig. 9. The difference in slope values between conditions (i) and (ii) is not significantly different at the 95% confidence interval, thus clearly demonstrating that Na^+ is mandatory for glucose transport in our preparation.

Discussion

Incompatibility with Two Independent Transporters

In this paper, we have reevaluated the kinetics of Na^+-D-glucose cotransport in rabbit jejunum brush border membrane vesicles. These studies were prompted by the development in our laboratory of a Fast Sampling, Rapid Filtration Apparatus (FSRFA) [3] which has allowed us to critically evaluate the limits of the rapid filtration technique and the problems associated with it for data analysis [4, 39]. Particular attention was also paid to the stability of the vesicle preparation [36], to the control of temperature, ionic strength, pH, and osmolarity in the transport assays, and to the first-order dependence of transport rates on protein concentrations. A major conclusion of our studies is that the kinetics of Na^+-D-glucose cotransport cannot be accounted for by the presence of two independent transporters, in contradiction with previous work on similar preparations [12, 25, 27]. A few comments are thus needed to fully appreciate the meaning of this fundamental difference.

A first issue deals with the assessment of true initial rates of transport. Obviously, as shown in Fig. 2 and the Table, the FSRFA allows us to solve that problem under all sets of experimental conditions by using either linear or polynomial regression analysis. Previous studies using rabbit intestinal brush border membrane vesicles were performed at 15°C [12] or room temperature [25, 27] and thus Fig. 2 should apply to these studies as well. Accordingly, for those studies where the initial rates were estimated at one time point of 2 sec [27] or 3 sec [25], it is quite clear that the initial rate assumption was fulfilled. For the study of Dorando and Crane [12], who pioneered the dynamic approach systematically applied with the FSRFA, four samples were collected over the range 5–15 sec, so that initial rate determinations had to be done from a polynomial regression analysis. Since this approach is justified by the experiment of Fig. 2 and the analysis in the Table (although using a higher number of data points equally spaced on the time axis), it would thus seem that the differences in conclusions between our investigation and other studies [12, 25, 27] might be more satisfactorily explained on other grounds.

A second issue deals with the experimental conditions used by the different groups for their kinetic studies in a similar preparation [12, 25, 27]. We have not tried to reproduce specifically any of these conditions. Instead, since the hypothesis that two Na^+-D-glucose cotransporters are present in the

small intestine relies on kinetic studies performed in different species and under different experimental conditions, we have systematically investigated some of the most representative situations and have devised our strategy to answer a number of critical issues. Starting with the standard conditions defined in the legend to Fig. 3, we thus: (i) compared two different methods for membrane potential clamping [2, 29]; (ii) explored the effect of a negative membrane potential (Fig. 6) which should have allowed comparison with Dorando and Crane's data [12]; (iii) lowered outside Na^+ concentrations (Fig. 5) to amplify a deviation from Michaelis-Menten behavior should a steady-state, random bi-bi order of substrate addition apply to a unique cotransporter (*see* Theory section 1*c* and [51]); (iv) increased outside Na^+ to 460 mM under negative membrane potential conditions (Fig. 7), a situation that seemed to increase the curvilinearity in the Eadie-Hofstee plots reported by Crane and Dorando [11] and may have helped in emphasizing negative cooperativity in a dimeric transporter (*see* Theory Section 1*c*); and (v) tested for a temperature effect under both zero-clamped and negative membrane potential values (Fig. 8) since temperature activation of a low-affinity carrier has been reported in the guinea pig small intestine [5]. It is thus remarkable that all of these experimental conditions failed to detect more than a pure Michaelis-Menten behavior. Moreover, the identical V_{max} obtained for D-glucose and D-galactose transport (Fig. 4) strongly support their sharing of a single carrier. Also, the demonstration that Na^+ is mandatory for transport (Fig. 9) rules out the possible existence of a low-affinity, Na^+-independent D-glucose transport system and of a low-affinity, Na^+-independent functioning mode of the cotransporter. Finally, it is worth noting that the K_m's determined in our studies are in the same range of values as those determined for SGLT1 when using α-methyl-D-glucose as substrate [47].

A last issue deals with the method used for kinetic data analysis since all previous studies in the rabbit small intestine made use of the Eadie-Hofstee plot. The observed deviations from linearity, however, were weak [27] or strong [12, 25] over a dynamic range of initial rate variations (i.e., over the range of cold substrate concentrations allowing for tracer displacement) similar to that of Figs. 2–8. Moreover, when looking back into these studies, it is not quite clear as to how the kinetic parameters were extracted and the statistical analyses, if any, performed. These difficulties seem to have been fully appreciated in one study [27] since the determination of kinetic parameters has not even been attempted. On the contrary, our studies have been specifically designed for model discrimination: (i) a wide range of substrate concentrations (12 or more) was used; (ii) the initial rate determinations were performed from the mean of five uptake time courses at each substrate concentration in order to allow for statistical analysis; (iii) the initial rate data were analyzed by weighted, nonlinear regression analysis according to displacement curves in order to avoid undue transformations in the error structure of the original measurements [4, 39]; and (iv) three model equations were systematically tested and statistically evaluated when performing the nonlinear regression analysis. It is quite remarkable, then, that none of the Eadie-Hofstee plots generated from the one-site, best-fit model in our different experimental conditions showed any sign of deviation from linearity.

We thus conclude that our data are compatible with the presence of only one transporter in the rabbit jejunum brush border membrane. We also conclude that the previous demonstration of two, kinetically separable, and independent Na^+-glucose cotransporters in this preparation is somehow related to the Eadie-Hofstee analysis of the kinetic data, in part for reasons similar to those previously discussed [39]. Our conclusions may not be extended to other species or tissues where a different situation may prevail. Nonetheless, considering that the present studies in the rabbit jejunum and our previous ones in the human small intestine [39] do conflict with reported observations on similar preparations, and that in both cases the best explanation for these discrepancies relates to the analytical part of the kinetic data, we think that caution should be the rule when the only evidence for transport heterogeneity comes from nonlinear Eadie-Hofstee plots. Moreover, as discussed in the Theory section, curvilinearity in such plots will not allow us to make the difference between the kinetic behavior of two independent transporters, random bi-bi mechanisms, and two interacting sites in a dimeric structure.

Implications for a Kinetic Mechanism of Na^+-D-Glucose Cotransport

The compatibility of Na^+-D-glucose cotransport with Michaelis-Menten kinetics neither excludes completely the presence of a second transporter nor does it yield any information concerning the monomeric or polymeric structure of the carrier protein. Should there be a second transporter, however, then it would have kinetic parameters and responsiveness to different physical and chemical situations which make it indistinguishable from the first—a probability that we rate as very low for two

independent carriers. Also, should there be only one monomeric transporter, then our results would conflict with previous kinetic studies demonstrating different coupling stoichiometries for Na^+/glucose cotransport [24–25, 37, 63] and partial inhibitions by a substrate analogue [19, 38] or inhibitor [38]. Moreover, this hypothesis will not account for the data of Koepsell et al. [31] showing that the equilibrium binding of phlorizin under Na^+-equilibrated conditions is heterogeneous with two classes of binding sites having identical B_{max}. The same restrictions hold true for polymeric transporters that may be reduced to a monomer-like kinetic mechanism, such as: (i) the subunits of the dimeric transporter behave independently; (ii) the negative cooperativity induced by the binding of the first substrate molecule is so high that it precludes the attachment of a second substrate molecule; and (iii) two subunits must combine to form a unique channel and one substrate binding site, contrary to one of our hypotheses of the Theory section.

It thus appears that the available kinetic evidence can only be reconciled by assuming a minimum of two substrate binding sites, and the question then arises as to what extent is such a hypothesis compatible with Michaelis-Menten kinetics. It should be noted first that the relative visibility of two interacting substrate binding sites, contrary to that of two independent transporters, will be constrained within a kinetic scheme and may not be affected by the experimental conditions. Also, in models like those of Fig. 1, transport through the CNa_2S and CNa_2S_2 complexes may occur at similar rates (*see* Theory section 2*c*). The problem thus amounts to resolving the following issue: would it be possible to get a kinetic separation of two carriers with the same V_{max} when using a radiotracer technique? As shown by Eq. (4) when setting $S_{cold} = 0$ and with $(T) \ll K_m$'s, the respective contribution of two transport pathways to total measured cpm is directly proportional to their V/K ratios, and two situations need to be considered: (i) the two sites have K_m ratios ≥ 10, in which case it can be calculated that the contribution of the low-affinity pathway to total measurable cpm will be $\leq 10\%$. Such a small contribution falls within the range of the experimental error (*see* Figs. 3–8) and, accordingly, the radiotracer technique is not appropriate for the kinetic separation; and (ii) the two sites have K_m ratios < 10, in which case their contribution to total measured cpm is significant but the small difference between the K_m values precludes their kinetic separation. We can thus conclude that the existence of two sites cannot be properly assessed at this time in models like those of Fig. 1 without further experiments demonstrating partial inhibition by a substrate analogue as performed by Malo in the human fetal small intestine [38] and confirming the existence of different stoichiometries of Na^+ : D-glucose cotransport at low and high substrate concentrations [25, 37]. Such experiments are now in progress in our laboratory.

A final comment should be made on the recently proposed homotetrameric structure of the cotransporter [56]. If the four subunits were to form a unique channel, as diagrammed by the authors [56] and acknowledged by Wright et al. [66] in a recent review, one would expect the kinetic manifestation of more than one substrate binding site in the most general case (Wright's group has indeed produced evidence for one Na^+ and one substrate binding site per polypeptide chain [49–50]). This model would thus be incompatible with our kinetic data. There is though a simple way to reconcile both the tetrameric structure of the transporter and the models of Fig. 1 by introducing the concept of half-of-the-sites reactivity, a mechanism that has always been found associated with negative cooperativity in substrate binding [33, 35, 44]. Accordingly, if we assume that the tetramer is formed by two pairs of functionally asymmetric subunits, so that one pair has an open channel facing the external membrane side, while the other one has its channel opened towards the inside, then none of the kinetic properties discussed for the dimers of Fig. 1 would be lost, at least under zero-*trans* conditions of both substrates. Moreover, the release of conformational energy induced by substrate binding to the outside-facing dimer could be transmitted to the inward-facing one in order to promote internal Na^+ and/or substrate release. Examples of such a functioning of the Na^+-D-glucose cotransporter, adapted to the published models of Kessler and Semenza [27] and Kimmich [28], are illustrated in Fig. 10. It is interesting to note that the principle of half-of-the-sites reactivity has also been applied recently to the mechanism of Na^+/H^+ antiport in the rabbit kidney [45]. As discussed in a theoretical paper from our group [65], however, the evidence for that mechanism in the latter study might not be that strong at this time. Nonetheless, such a functioning of the Na^+-D-glucose cotransporter is quite appealing as it would solve the problem of "leak" pathways [8], propose a rational explanation to the "valve" effects and the problem of energy transfer from an ionic gradient to a cotransporter protein as discussed by Crane [8], and answer the question raised by Kimmich when presenting his most recent model [28]: "the fully loaded carrier must undergo a conformational change that allows access of bound sol-

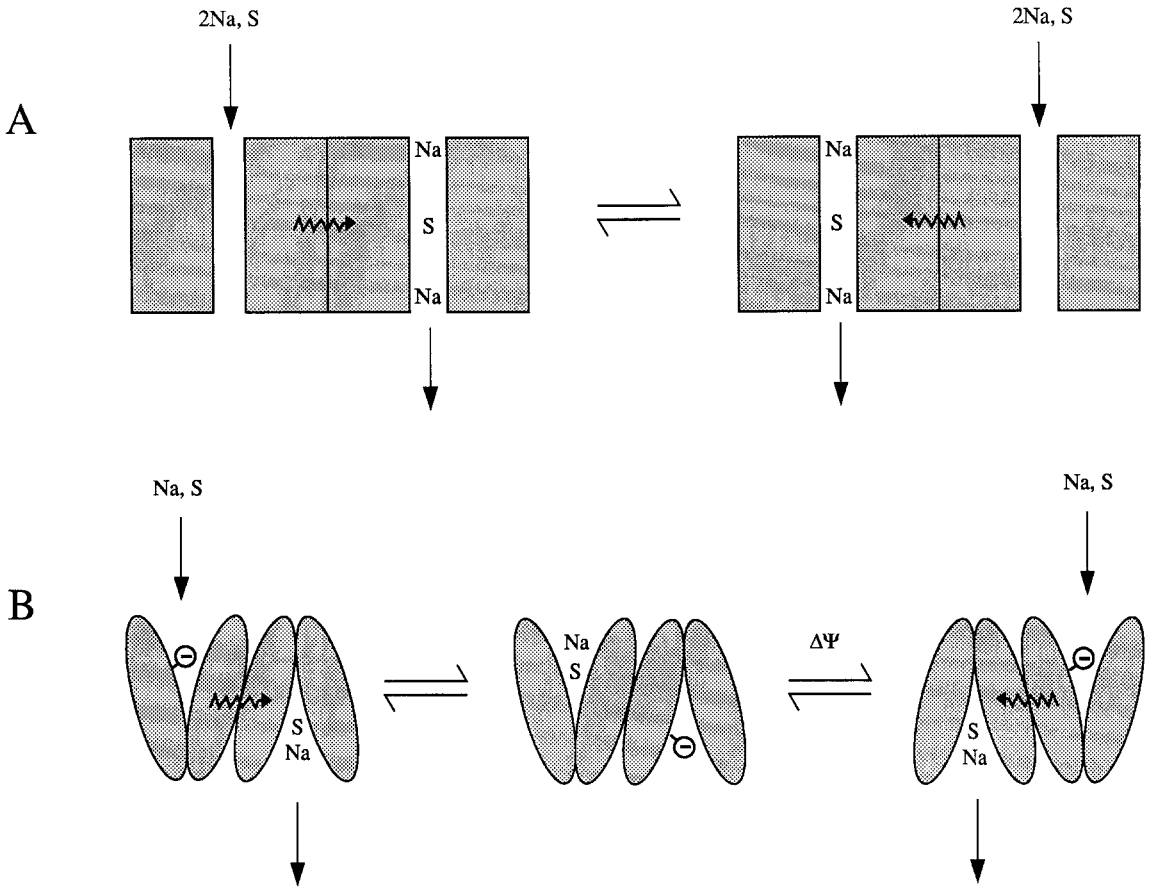

Fig. 10. Possible tetrameric models for Na^+-D-glucose cotransport showing negative cooperativity for substrate binding to the transporter: (*A*) application to Kimmich's model [28]; (*B*) application to the asymmetric gated channel responsive to $\Delta\Psi$ proposed by Kessler and Semenza [27]. In both cases, the transporter is viewed as a functionally asymmetric structure in which the basic functional units are dimers. Under steady-state (or physiological) conditions, free binding sites are outwardly oriented. Positive cooperativity for Na^+ binding allows for energy transduction from the Na^+ electrochemical gradient to the transporter under the form of conformational energy which can then be released by the negative cooperativity induced upon glucose (S) binding. This energy (arrows) can then be transmitted to the neighboring subunit, allowing for Na^+ and/or substrate release on the inside. In *A*, this step is sufficient to allow for a new cycle of transport. In *B*, the negative charge of the inside-facing dimer can now sense the membrane potential and thus allow for site reorientation as proposed by Kessler and Semenza [27]. *See also* text for further comments and justifications.

utes to the intracellular compartment while at the same time excluding further entry of solutes from outside."

This research was supported by grant MT-7607 from the Medical Research Council of Canada. One of the authors (A.B.) was supported by a scholarship from the "Fonds de la Recherche en Santé du Québec" and C. C. was supported by a fellowship from the GRTM. The technical assistance of Mrs. C. Leroy has been greatly appreciated. The authors also thank D.D. Maenz and C. Malo for insightful discussions and C. Gauthier for the art work.

References

1. Berteloot, A. 1984. Characteristics of glutamic acid transport by rabbit intestinal brush-border membrane vesicles. Effects of Na^+-, K^+-, and H^+- gradients. *Biochim. Biophys. Acta* **775**:129–140
2. Berteloot, A. 1986. Highly permeant anions and glucose uptake as an alternative for quantitative generation and estimation of membrane potential differences in brush border membrane vesicles. *Biochim. Biophys. Acta* **775**:129–140
3. Berteloot, A., Malo, C., Breton, S., Brunette, M. 1991. A fast sampling, rapid filtration apparatus: principal characteristics and validation from studies of D-glucose transport in human jejunal brush-border membrane vesicles. *J. Membrane Biol.* **122**:111–125
4. Berteloot, A., Semenza, G. 1990. Advantages and limitations of vesicles for the characterization and the kinetic analysis of transport systems. *Meth. Enzymol.* **192**:409–437
5. Brot-Laroche, E., Serrano, M., Delhomme, B., Alvarado, F. 1986. Temperature sensitivity and substrate specificity of two distinct Na^+-activated D-glucose transport systems in guinea pig jejunal brush border membrane vesicles. *J. Biol. Chem.* **261**:6168–6176

6. Centelles, J.J., Kinne, R.K.H., Heinz, E. 1991. Energy coupling of Na-glucose cotransport. *Biochim. Biophys. Acta* **1065:**239–249
7. Coady, M.J., Pajor, A.M., Wright, E.M. 1990. Sequence homologies among intestinal and renal Na^+/glucose cotransporters. *Am. J. Physiol.* **259:**C605–C610
8. Crane, R.K. 1977. The gradient hypothesis and other models of carrier-mediated active transport. *Rev. Physiol. Biochem. Pharmacol.* **78:**99–159
9. Crane, R.K. 1985. Comments and experiments on the kinetics of Na^+ gradient-coupled glucose transport as found in rabbit jejunal brush-border membrane vesicles. *Ann. N. Y. Acad. Sci.* **456:**36–46
10. Crane, R.K., Dorando, F.C. 1979. On the mechanism of Na^+-dependent glucose transport. *In:* Functional and Molecular Aspects of Biomembrane Transport. E. Quagliariello et al., editors. pp. 271–278. Elsevier/North-Holland Biomedical, Amsterdam
11. Crane, R.K., Dorando, F.C. 1982. The kinetics and mechanism of Na^+ gradient-coupled transport. *In:* Membranes and Transport. A. Martonosi, editor. Vol. 2, pp. 153–160. Plenum, New York
12. Dorando, F.C., Crane, R.K. 1984. Studies of the kinetics of Na^+ gradient coupled glucose transport as found in brush-border membrane vesicles from rabbit jejunum. *Biochim. Biophys. Acta* **772:**273–287
13. Dudeja, P.K., Wali, R.K., Klitzke, A., Brasitus, T.A. 1990. Intestinal D-glucose transport and membrane fluidity along crypt-villus axis of streptozocin-induced diabetic rats. *Am. J. Physiol.* **259:**G571–G577
14. Freeman, H.J., Johnston, G., Quamme, G.A. 1987. Sodium-dependent D-glucose transport in brush-border membrane vesicles from isolated rat small intestinal villus and crypt epithelial cells. *Can. J. Physiol. Pharmacol.* **65:**1213–1219
15. Freeman, H.J., Quamme, G.A. 1986. Age-related changes in sodium-dependent glucose transport in small intestine. *Am. J. Physiol.* **251:**G208–G217
16. Harig, J.M., Barry, J.A., Rajendran, V.M., Soergel, K.H., Ramaswamy, K. 1989. D-glucose and L-leucine transport by human intestinal brush-border membrane vesicles. *Am. J. Physiol.* **256:**G618–G623
17. Harrison, D., Rowe, G., Lumsden, C.J., Silverman, M. 1984. Computational analysis of models for cotransport. *Biochim. Biophys. Acta* **774:**1–10
18. Hediger, M.A., Coady, M.J., Ikeda, T.S., Wright, E.M. 1987. Expression cloning and cDNA sequencing of the Na^+/glucose cotransporter. *Nature* **330:**379–381
19. Honegger, P., Semenza, G. 1973. Multiplicity of carriers for free glucalogues in hamster small intestine. *Biochim. Biophys. Acta* **318:**390–410
20. Hopfer, U. 1981. Kinetic criteria for carrier-mediated transport mechanisms in membrane vesicles. *Fed. Proc.* **40:**2480–2485
21. Hopfer, U., Nelson, K., Perrotto, J., Isselbacher, K.J. 1973. Glucose transport in isolated brush border membranes from rat small intestine. *J. Biol. Chem.* **248:**25–32
22. Hwang, E., Hirayama, B., Wright, E.M. 1991. Distribution of the SGLT1 Na^+/glucose cotransporter and mRNA along the crypt-villus axis of rabbit small intestine. *Biochem. Biophys. Res. Commun.* **181:**1208–1217
23. Karasov, W.H., Diamond, J.M. 1983. Adaptative regulation of sugar and amino acid transport by vertebrate intestine. *Am. J. Physiol.* **245:**G443–G462
24. Kaunitz, J.D., Gunther, R., Wright, E.M. 1982. Involvement of multiple sodium ions in intestinal D-glucose transport. *Proc. Natl. Acad. Sci. USA* **79:**2315–2318
25. Kaunitz, J.D., Wright, E.M. 1984. Kinetics of sodium D-glucose cotransport in bovine intestinal brush border vesicles. *J. Membrane Biol.* **79:**41–51
26. Keljo, D.J., MacLeod, R.J., Perdue, M.H., Butler, D.G., Hamilton, J.R. 1985. D-glucose transport in piglet jejunal brush border membranes: insights from a disease model. *Am. J. Physiol.* **249:**G751–G760
27. Kessler, M., Semenza, G. 1983. The small-intestinal Na^+, D-glucose cotransporter: An asymmetric gated channel (or pore) responsive to $\Delta\Psi$. *J. Membrane Biol.* **76:**27–56
28. Kimmich, G.A. 1990. Membrane potentials and mechanism of intestinal Na^+-dependent sugar transport. *J. Membrane Biol.* **114:**1–27
29. Kimmich, G.A., Randles, J., Restrepo, D., Montrose, M. 1985. A new method for determination of relative ion permeabilities in isolated cells. *Am. J. Physiol.* **248:**C399–C405
30. Kinne, R., Da Cruz, M.E.M., Lin, J.T. 1984. Sodium-D-glucose cotransport system. Biochemical analysis of active sites. *Curr. Top. Membr. Trans.* **20:**245–258
31. Koepsell, H., Fritzsch, G., Korn, K., Madrala, A. 1990. Two substrate sites in the renal Na^+-D-glucose cotransporter studied by model analysis of phlorizin binding and D-glucose transport measurements. *J. Membrane Biol.* **114:**113–132
32. Koshland, D.E., Jr., Nemethy, G., Filmer, D. 1966. Comparison of experimental binding data and theoretical models in protein containing subunits. *Biochemistry* **5:**365–385
33. Lazdunski, M. 1972. Flip-flop mechanisms and half-site enzymes. *Curr. Top. Cell. Regul.* **6:**267–309
34. Levitzki, A. 1978. Quantitative aspects of allosteric mechanisms. *Molec. Biol. Biochem. Biophys.* **28:**1–104
35. Levitzki, A., Koshland, D.E., Jr. 1976. The role of negative cooperativity and half-of-the-sites reactivity in enzyme regulation. *Curr. Top. Cell. Regul.* **10:**1–40
36. Maenz D.D., Chenu, C., Bellemare, F., Berteloot, A. 1991. Improved stability of rabbit and rat intestinal brush border membrane vesicles using phospholipase inhibitors. *Biochim. Biophys. Acta* **1069:**250–258
37. Malo, C. 1988. Kinetic evidence for heterogeneity in Na^+-D-glucose cotransport systems in the normal human fetal small intestine. *Biochim. Biophys. Acta* **938:**181–188
38. Malo, C. 1990. Separation of two distinct Na^+/D-glucose cotransport systems in the human fetal jejunum by means of their differential specificity for 3-O-methylglucose. *Biochim. Biophys. Acta* **1022:**8–16
39. Malo, C., Berteloot, A. 1991. Analysis of kinetic data in transport studies: new insights from kinetic studies of Na^+-D-glucose cotransport in human intestinal brush-border membrane vesicles using a fast sampling, rapid filtration apparatus. *J. Membrane Biol.* **122:**127–141
40. Mannervik, B. 1981. Design and analysis of kinetic experiments for discrimination between rival models. *In:* Kinetic Data Analysis. Design and Analysis of Enzyme and Pharmacokinetic Experiments. L. Endrenyi, editor. pp 235–270. Plenum, New York and London
41. Monod, J, Wyman, J., Changeux, J.-P. 1965. On the nature of allosteric transitions: a plausible model. *J. Mol. Biol.* **12:**88–118
42. Morrison, A.I., Panayotova-Heiermann, M., Feigl, G., Schlölermann, B., Kinne, R.K.H. 1991. Sequence comparison of the sodium-D-glucose cotransport systems in rabbit

renal and intestinal epithelia. *Biochim. Biophys. Acta* **1089:**121–123
43. Murer, H., Biber, J., Gmaj, P., Stieger, B. 1984. Cellular mechanisms in epithelial transport: advantages and disadvantages of studies with vesicles. *Mol. Physiol.* **6:**55–82
44. Neet, K.E. 1980. Cooperativity in enzyme function: equilibrium and kinetic aspects. *Meth. Enzymol.* **64:**139–192
45. Otsu. K., Kinsella, J., Sacktor, B., Froehlich, J.P. 1989. Transient state kinetic evidence for an oligomer in the mechanism of Na^+-H^+ exchange. *Proc. Natl. Acad. Sci. USA* **86:**4818–4822
46. Pajor, A., Hirayama, B.A., Wright, E.M. 1992. Molecular evidence for two renal Na^+/glucose transporters. *Biochim. Biophys. Acta* **1106:**216–220
47. Parent, L., Supplisson, S., Loo, D.D.F., Wright, E.M. 1992. Electrogenic properties of the cloned Na^+/Glucose cotransporter: I. Voltage-clamp studies. *J. Membrane Biol.* **125:**49–62
48. Parent, L., Supplisson, S., Loo, D.D.F., Wright, E.M. 1992. Electrogenic properties of the cloned Na^+/Glucose cotransporter: II. A transport model under nonrapid equilibrium conditions. *J. Membrane Biol.* **125:**63–79
49. Peerce, B.E., Wright, E.M. 1985. Evidence for hydroxyl residues at the Na^+ site on the intestinal Na^+-glucose cotransporter. *J. Biol. Chem.* **260:**6026–6031
50. Peerce, B.E., Wright, E.M. 1986. Distance between substrate sites on the Na-glucose cotransporter by fluorescence energy transfer. *Proc. Natl. Acad. Sci. USA* **83:**8092–8096
51. Sanders, D. 1986. Generalized kinetic analysis of ion-driven cotransport systems: II. Random ligand binding as a simple explanation for non-Michaelian kinetics. *J. Membrane Biol.* **90:**67–87
52. Schmidt, U.M., Eddy, B., Fraser, C.M., Venter, J.C., Semenza, G. 1983. Isolation of (a subunit of) the Na^+/D-glucose cotransporter(s) of rabbit intestinal brush-border membranes using monoclonal antibodies. *FEBS Lett.* **161:**279–283
53. Schmitz, J., Preiser, H., Maestracci, D., Ghosh, B.K., Cerda, J.J., Crane, R.K. 1973. Purification of the human intestinal brush border membrane. *Biochim. Biophys. Acta* **323:**98–112
54. Semenza, G., Kessler, M., Hosang, M., Weber, J., Schmidt, U. 1984. Biochemistry of the Na^+-D-glucose cotransporter of the small-intestinal brush-border membrane. *Biochim. Biophys. Acta* **779:**343–379
55. Silverman, M. 1991. Structure and function of hexose transporters. *Annu. Rev. Biochem.* **60:**757–794
56. Stevens, B.R., Fernandez, A., Hirayama, B., Wright, E.M., Kempner, E.S. 1990. Intestinal brush border membrane Na^+/glucose cotransporter functions in situ as a homotetramer. *Proc. Natl. Acad. Sci. USA* **87:**1456–1460
57. Takata, K., Kasahara, T., Kasahara, M., Ezaki, O., Hirano, H. 1991. Localization of Na^+dependent active type and erythrocyte/HepG2-type glucose transporters in rat kidney: Immunofluorescence and immunogold study. *J. Histochem. Cytochem.* **39:**287–298
58. Takata, K., Kasahara, T., Kasahara, M., Ezaki, O., Hirano, H. 1992. Immunohistochemical localization of Na^+-dependent glucose transporter in rat jejunum. *Cell Tissue Res.* **267:**3–9
59. Turk, E., Zabel, B., Mundlos, S., Dyer, J., Wright, E.M. 1991. Glucose/galactose malabsorption caused by a defect in the Na^+/glucose cotransporter. *Nature* **350:**354–356
60. Turner, R.J. 1983. Quantitative studies of cotransport systems: models and vesicles. *J. Membrane Biol.* **76:**1–15
61. Turner, J. 1985. Solution of carrier-type transport models: General solution for an arbitrarily complex rapid equilibrium model. *J. Membrane Biol.* **88:**77–83
62. Turner, R.J., Moran, A. 1982. Heterogeneity of sodium-dependent D-glucose transport sites along the proximal tubule: evidence from vesicle studies. *Am. J. Physiol.* **242:**F406–F414
63. Turner, R.J., Moran, A. 1982. Stoichiometric studies of the renal outer cortical brush border membrane D-glucose transporter. *J. Membrane Biol.* **67:**73–80
64. Turner, R.J., Moran, A. 1982. Further studies of proximal tubular brush border membrane D-glucose transport heterogeneity. *J. Membrane Biol.* **70:**37–45
65. Wierzbicki, W., Berteloot, A., Roy, G. 1990. Presteady-state kinetics and carrier-mediated transport: a theoretical analysis. *J. Membrane Biol.* **117:**11–27
66. Wright, E.M., Turk, E., Zabel, B., Mundlos, S., Dyer, J. 1991. Molecular genetics and intestinal glucose transport. *J. Clin. Invest.* **88:**1435–1440

Received 3 March 1992; revised 28 September 1992